Available online at www.sciencedirect.com
ScienceDirect
Trans. Nonferrous Met. Soc. China 25(2015) 1383−1390
Transactions of Nonferrous Metals Society of China
www.tnmsc.cn

Effect of pre-deformation on aging creep of Al−Li−S4 alloy and its constitutive modeling

Meng WANG[1,2], Li-hua ZHAN[1,2], You-liang YANG[1,2], Ling YANG[1,2], Ming-hui HUANG[1,2]

1. School of Mechanical and Electrical Engineering, Central South University, Changsha 410083, China;
2. State Key Laboratory of High Performance Complex Manufacturing, Central South University, Changsha 410083, China

Received 24 May 2014; accepted 27 February 2015

Abstract: A set of uniaxial tensile creep tests at different pre-deformations, aging temperatures and stress levels were carried out for Al−Li−S4 alloy, and the creep behavior and the effects of pre-deformation on mechanical properties and microstructures were determined under basic thermodynamics conditions of aging forming. The results show that pre-deformation shortens the time of primary creep and raises the second steady-state creep rate. Then, the total creep strain is greater, but in the range of test parameters it is still smaller than that without pre-deformation. In addition, transmission electron microscopy (TEM) observation shows that pre-deformation promotes the formation of $T1$ phase and θ' phase and makes them distribute more dispersively, while inhibits the generation of δ' phase, which leads to the improvement of mechanical properties of the alloy. A unified constitutive model reflecting the effects of aging mechanism, stress levels and different pre-deformations was established. The fitting results agree with the experimental data well.

Key words: Al−Li−S4 alloy; aging creep; pre-deformation; mechanical properties; microstructure; constitutive model

1 Introduction

Creep age forming (CAF) makes use of age hardening characteristic and creep formation feature of materials to acquire the satisfied shape and properties during workpiece forming, and it is advantageous for manufacturing large integral panels with reinforced ribs and complex curvatures [1−3]. CAF is considered one of the most important forming methods in manufacturing aircraft integral panels and has broad application prospects in the development of large passenger planes, military transport aircrafts and high-speed aerospace rockets [4−6].

According to relevant researches, pre-deformation before aging treatment can raise the dislocation density in the alloy, reduce the size of precipitates and shorten the time for the peak-aged. In this way, the alloy can meet satisfied strength with good plasticity, toughness and stress corrosion cracking resistance, which has better integrated performances than the alloy after sole cold working or artificial aging. In the test studies and actual processes, the thermo-mechanical treatment process including solid solution, quenching, cold deformation and artificial aging is used as a significant measure to improve the integrated performance of the alloy. However, the researches on pre-deformation of aluminum alloy are mainly focused on how to improve microstructures or mechanical properties [7−10]. There are less studies concerning the effect of pre-deformation on aging creep behavior and comprehensive properties of material, and unified creep constitutive model describing the effect of pre-deformation. This situation makes it difficult to accurately control process parameters and predict springback in the CAF process.

In recent decades, Al−Li alloys have been developed rapidly due to their high elasticity modulus, low density, good fatigue, stress corrosion resistance and many other excellent performances. Al−Li alloys have been regarded as one of the best light mass and high strength structural materials in aerospace industry [11−14] and are widely used in the fuselages, wings and other important structures of aircrafts. Al−Li−S4 alloy is a new kind of Al−Li−Cu alloy which was developed for

Foundation item: Project (2014CB046602) supported by the National Basic Research Program of China; Project (51235010) supported by the National Natural Science Foundation of China
Corresponding author: Li-hua ZHAN; Tel: +86-731-88830254; E-mail: yjs-cast@csu.edu.cn
DOI: 10.1016/S1003-6326(15)63737-2

large passenger aircrafts by Alcoa recently. And the technological parameters for producing this alloy are still technology secrets, but its strength, ductility and toughness can be enhanced by artificial aging [15].

From the above, it has huge research and engineering significance to use Al−Li−S4 alloy as the experimental material. This research consists of experimental studies and creep constitutive model under CAF conditions. Firstly, the overall experimental programme was introduced. Secondly, the rule of creep behaviors and the effects of pre-deformation on its mechanical properties and microstructure were determined by analyzing the experimental results. Lastly, a unified creep constitutive model which can reflect the influences of aging mechanism, stress levels and pre-deformation was established by modifying Kowalewski's equations. This work could provide certain support for the manufacturing of large integral panels and the development of CAF technology about Al−Li−S4 alloy.

2 Experimental

The specific chemical composition of Al−Li−S4 alloy is shown in Table 1. The test samples were prepared according to the Standard of ISO 204−1997 (Metallic materials−uniaxial creep testing intension−Method of test). The dimensions of samples are 100 mm in gauge length and 2 mm in thickness, as illustrated in Fig. 1.

Table 1 Composition of Al−Li−S4 alloy (mass fraction, %)

Si	Fe	Cu	Mn	Mg	Zn
0.014	0.028	3.64	0.29	0.71	0.36
Ag	Li	Zr	Ti	Al	
0.32	0.68	0.12	0.026	Bal.	

In this work, the heat treatment procedure for Al−Li−S4 alloy was obtained by differential scanning calorimetry (DSC). The DSC test was conducted for sample of 12.458 mg using SDT−Q600 instrument. The DSC curves are shown in Fig. 2.

In Fig. 2(b), two endothermic peaks appear at 525 and 550 °C. The alloy liquidus is at 640 °C and the melting temperature range of non-equilibrium low-melting eutectic phase is 525−550 °C. By the analysis of DSC curves, coupled with Chinese Standard YS/T591−

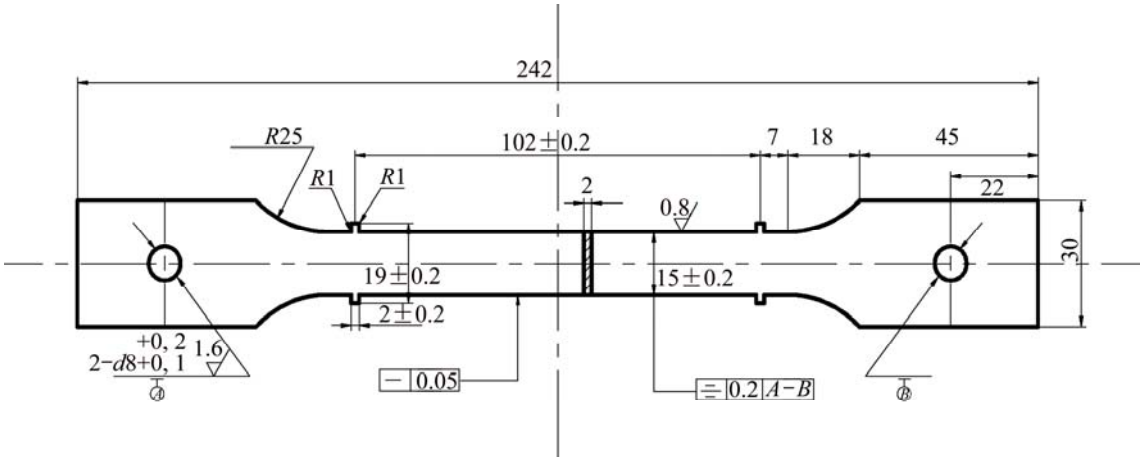

Fig. 1 Schematic of aging creep sample for Al−Li−S4 alloy (unit: mm)

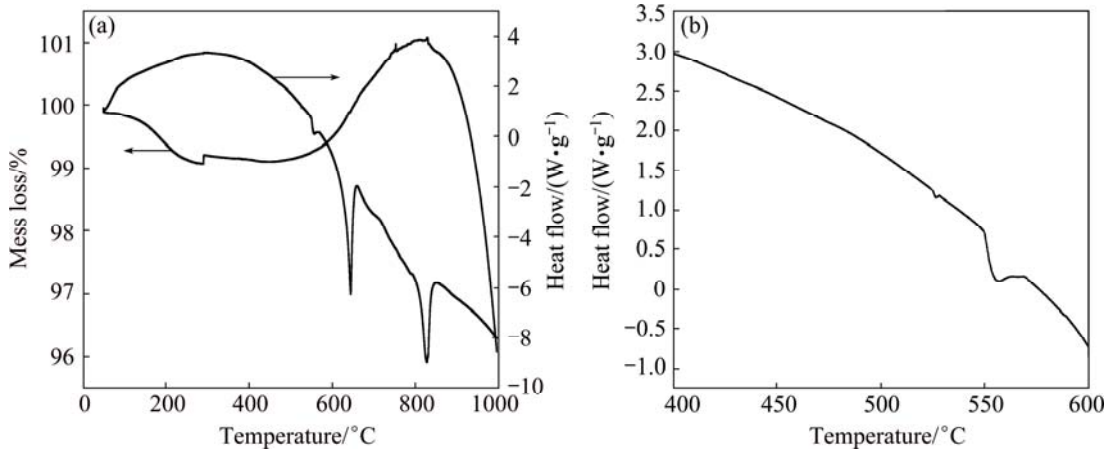

Fig. 2 DSC curves for Al−Li−S4 alloy: (a) Whole curve; (b) Magnification of heat flow near 525 and 550 °C

2006 (Wrought aluminum and aluminum alloys heat treatment), the temperature for solution-treatment is defined at (520±3) °C. This result agrees with the results in Refs. [16−18] on Al−Li−S4 alloy or other Al−Li alloys. The samples were subjected to water quenching after solution heat-treatment at 520 °C for 50 min, and the transfer time from furnace to water should be less than 35 s. Then, a set of creep tests were performed on the RDL50 electronic creep testing machine under temperatures of 175−195 °C, stress levels of 160−200 MPa, and pre-deformations of 0−5%.

The conductivity of samples after test was measured on a 7501A eddy current conductivity meter. The hardness was determined on an HXD−1000TM/LCD digital micro hardness tester. In the hardness test, the load was set to be 29.4 N and the loading time was 15 s. The conductivity and hardness of five different positions on each simple were taken and then their average values were gotten. Then the variation of yield strength was analyzed through hardness change. Transmission electron microscopy (TEM) samples were first ground and polished to 60 um in thickness, and then twin-jet electropolished using 75% methanol and 25% nitric acid solution. In the end, TEM samples were observed on a Tecnai F30G transmission electron microscope.

3 Results and discussion

3.1 Effect of pre-deformation on aging creep behaviors

Figure 3 describes the aging creep curves of Al−Li−S4 alloy under conditions of different temperatures, stress levels and pre-deformations. It can be clearly seen that Al−Li−S4 alloy exhibits typical features of the primary and secondary creep stages, and even more than 70% of the total creep strain of samples without pre-deformation is contributed to the first creep stage under 185 °C, 180 MPa and without pre-deformation. As illustrated in Fig. 3(c), the creep strain of samples without pre-deformation is greater than that of the ones with pre-deformation. Pre-deformation can obviously shorten the first creep stage and raise the steady creep rate. The larger the amount of pre-deformation is, the greater the effects on creep behaviors are, and then the larger the total creep strain is.

It can be observed that the creep rate of primary stage decreases in contrast with samples without pre-deformation. This is ascribed to the two reasons. Firstly, due to pre-deformation before creep, a large number of defects such as dislocations and vacancies are produced in the matrix, and then promote the second phase precipitating, which helps to hinder dislocation motions. Secondly, pre-deformation brings about work-hardening

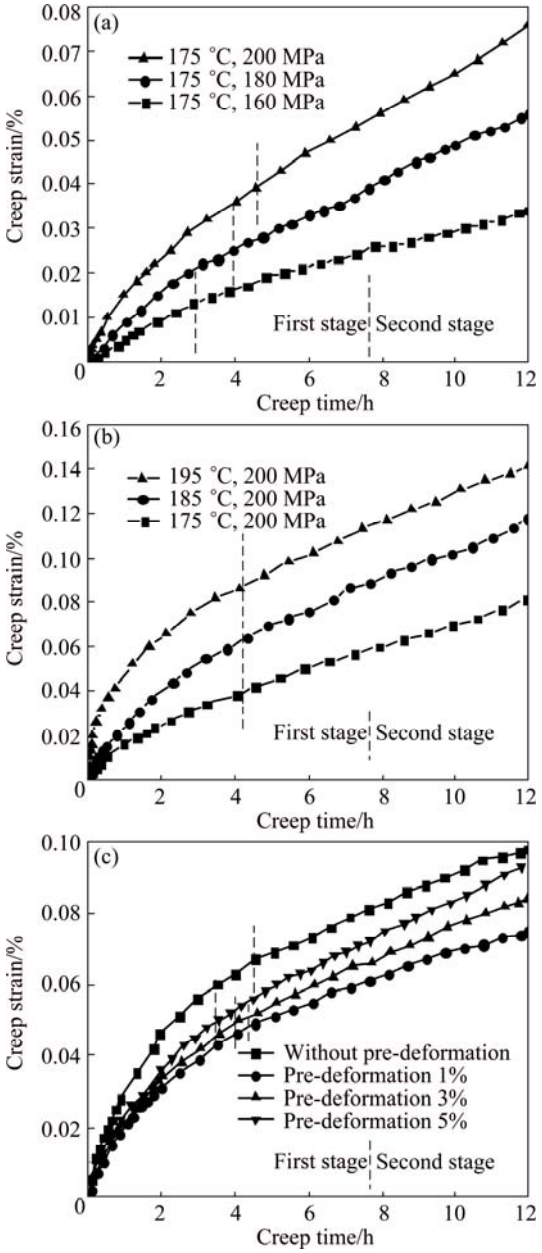

Fig. 3 Creep curves of Al−Li−S4 alloy under different conditions: (a) Under the same temperature, different stress levels and without pre-deformation; (b) Under the same stress, different temperatures and without pre-deformation; (c) Under 185 °C and 180 MPa but different pre-deformations

phenomenon; thereby, internal dislocation pile-ups and more precipitates keep creep strain from going on. On the other hand, as more dislocations exist in the secondary creep stage due to pre-deformation, it is easier to generate dislocation slip and climb. This results in the increase of steady creep rate.

3.2 Effect of pre-deformation on mechanical properties

Figure 4 shows that the hardness of material varies with pre-deformation after aging creep at 185 °C and

180 MPa for 12 h. As seen from Fig. 4, the samples exhibit relatively high level of hardness after tests, and the hardness increases linearly with increasing pre-deformation from 0 to 5%.

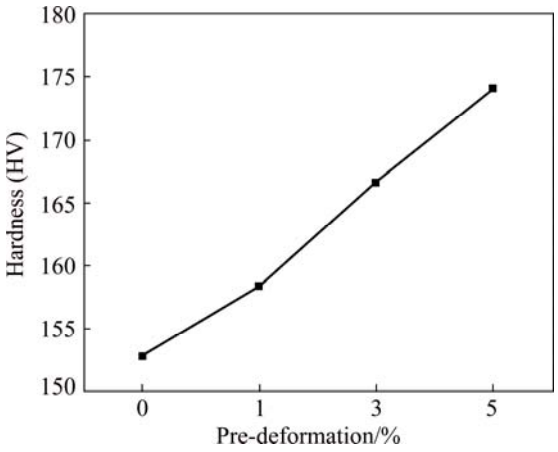

Fig. 4 Variation of hardness of Al−Li−S4 alloy with pre-deformation after aging creep at 185 °C and 180 MPa for 12 h

Aging creep can obviously strengthen the material and hence improve hardness of material greatly [19]. Besides, numerous dislocations and dislocation tangle appear due to pre-deformation prior to aging creep, which cause work-hardening effect. Furthermore, in the range of test parameters, higher pre-deformation leads to higher level of dislocation density. So, the macroscopic hardness increases linearly.

Relevant researches [20−22] indicate that there is a strongly linear relationship between metal hardness and strength, which can be described approximately as follows:

$$\sigma_b=KH-D \quad (1)$$

where σ_b is the tensile strength, H is the material hardness, K and D are material constants. For aluminum alloys, K lies within the range from 2.7 to 3.8, and D can be set to be 0. From Eq. (1), it can be concluded that the tensile strength of Al−Li−S4 alloy monotonously increases with pre-deformation when maintaining other process parameters identical.

The conductivity−pre-deformation curve of Al−Li−S4 alloy after aging creep (185 °C, 180 MPa, 12 h) is shown in Fig. 5. As seen from Fig. 5, within a certain range of pre-deformation, conductivity increases gradually but slightly.

Aluminum substrate, solid-solution atoms or atom-cluster, and precipitates mainly contribute to the conductivity of the alloy, and in creep forming the change of conductivity can reflect the precipitating behaviors. As the precipitating behaviors affect mechanical properties of the alloy such as hardness and strength, researches on the change rules of conductivity

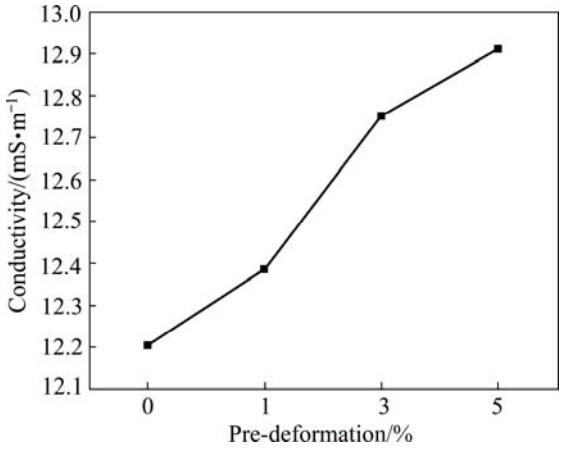

Fig. 5 Variation of conductivity with pre-deformation after aging creep at 185 °C and 180 MPa for 12 h for Al−Li−S4 alloy

in the process of aging creep and the relationship between conductivity and strength are helpful and useful to realize the concurrent change of mechanical properties and their changing mechanisms. Specifically for the effect of pre-deformation, vacancies and dislocations produced by pre-deformation provide more advantageous sites for precipitate nucleation and also have a positive effect on their growth. As a result, the volume fraction of precipitates increases and conductivity follows to rise.

3.3 Effect of pre-deformation on microstructures

Figure 6 shows TEM bright field images showing the changes of matrix precipitates (MPt) of samples with various pre-deformations after aging creep at 185 °C and 180 MPa for 12 h. The TEM images of the corresponding grain boundary precipitates (GBP) are shown in Fig. 7.

For samples without pre-deformation (see Figs. 6(a) and 7(a)), slender acicular θ' phase (Al_2Cu), rod-like $T1$ phase (Al_2CuLi) and spherical δ' phase (Al_3Li) can be found in grains or at grain boundaries. However, the quantity and distribution of these precipitates in samples with different pre-deformations are different. In Fig. 6, with the increase of pre-deformation, there are more and finer θ' phase and $T1$ phase distributing dispersively in grains, but δ' phase gradually decreases and eventually disappears. The reason is that lots of dislocations and dislocation tangle are brought into the alloy matrix due to the cold deformation before aging creep. These defects can provide advantageous nucleation sites for θ' phase and $T1$ phase, and then promote their fine dispersion. It is generally believed that, in Al−Li−S4 alloy, θ' phase is metastable phase and $T1$ phase is equilibrium phase. Therefore, the variation of volume free energy needed to form $T1$ phase is greater than that of θ' phase. Meanwhile, dislocations produced by pre-deformation may become

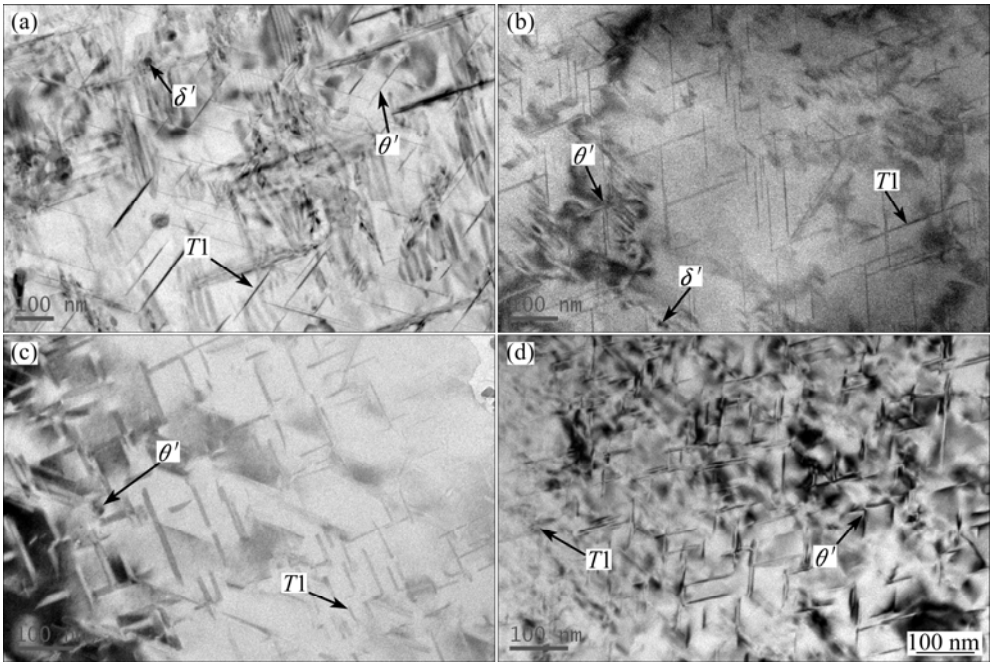

Fig. 6 TEM bright field images for matrix precipitates of Al−Li−S4 alloy after pre-deformation and aging creep (185 °C, 180 MPa, 12 h): (a) Without pre-deformation; (b) Pre-deformation 1%; (c) Pre-deformation 3%; (d) Pre-deformation 5%

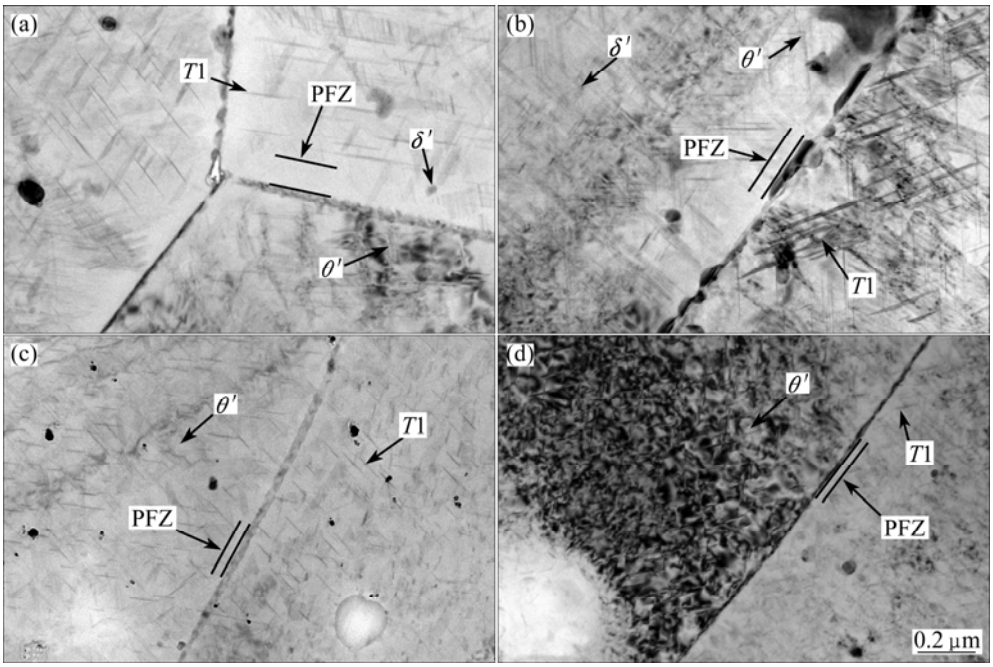

Fig. 7 TEM bright field images for grain boundary precipitates of Al−Li−S4 alloy after pre-deformation and aging creep (185 °C, 180 MPa, 12 h): (a) Without pre-deformation; (b) Pre-deformation 1%; (c) Pre-deformation 3%; (d) Pre-deformation 5%

the trap for vacancy annihilation. This results in a decrease of vacancies, which inhibits the precipitation of θ'' phase and θ' phase. According to the results described above, pre-deformation has a more promoting effect on $T1$ phase than θ' phase. Nevertheless, as Cu content is 5−6 times of Li content in Al−Li−S4 alloy, there is still a certain amount of θ' phase in spite of the existence of dislocations in grains. Moreover, both of coherent strain energy and interface energy between δ' phase and aluminum matrix are relatively low, δ' phase tends to appear in the form of homogeneous nucleation, so, the quantity and morphology of δ' phase cannot be influenced by pre-deformation. However, because the growth of $T1$ phase depletes Li atoms in the solid solution, δ' phase dissolves and even disappears.

With regard to Fig. 7(a), there are obvious precipitate free zones (PFZ) around the grain boundaries of sample without pre-deformation and the precipitates at

grain boundaries are chain-like. As the pre-deformation increases, PFZs become narrower and the chain-like precipitates at grain boundaries distribute more and more continuously. These continuous precipitates at grain boundaries are very detrimental to the plasticity and toughness of alloy because they can impede the motion of grains deformation [23−25]. Meanwhile, *T*1 phase always precipitates in the way of nonuniform nucleation at grain defects, such as dislocations, subgrain boundaries and grain boundaries. The increase of pre-deformation also makes dislocation density arising and so disperses T_1 phase from grain boundaries to more places, especially among dislocations in grains. While θ' phase mainly precipitates at the position where dislocations congregate and strongly pins the dislocations.

Considering the combined effects of pre-deformation on grains and grain boundaries, suitable pre-deformation is required to be given to obtain desired mechanical properties after aging creep.

4 Unified creep constitutive model

4.1 Establishment of model

Researchers [26−28] came up with the unified creep damage constitutive model about aluminum alloys based on the unified theory and aging dynamics. This model was obtained by combining material stress−strain relationship with microstructure evolution, such as second-phase precipitation and grain growth. It could describe the creep behaviors from the primary stage to the tertiary stage, possessing considerable scientific significance and great engineering guidance value [27,28].

In fact, the aging time is fairly short in the process of CAF, and materials will not show the tertiary-creep-stage behavior. Therefore, when establishing the unified creep constitutive model for Al−Li−S4 alloy it is necessary to focus on describing properties of aging creep but ignore the part about tertiary-creep-stage for simplification. Besides, the influence of pre-deformation on alloys originates mainly from dislocation mechanism [8,29]. In order to explain clearly, the creep constitutive model is described as follows:

$$\dot{\varepsilon} = A\sinh[B(\sigma-\sigma_0)(1-H)^{m_0}(1+\frac{Y}{Y^*})^{n_0}]\exp(-\frac{Q}{RT}) \quad (2)$$

$$\dot{H} = \frac{h}{\sigma^{m_1}}(1-\frac{H}{H^*})(1+\frac{Y}{Y^*})^{n_1}\dot{\varepsilon} \quad (3)$$

where A, B, h, H^*, m_0, m_1, n_0 and n_1 are material constants; Q represents the creep apparent activation energy; R is the gas molar constant; T is the aging temperature; Y is the amount of current pre-deformation; Y^* is the amount of ultimate pre-deformation.

In Eq. (3), H^* describes the varying rate of dislocation strengthening which reflects work-hardening influence and mainly controls the strain rate of the first creep stage, and it is the limit of dislocation strengthening. Due to inhibiting effect of pre-deformation at the first creep stage, mathematical description is embodied in Eq. (3). In Eq. (2), σ_0 describes the creep threshold stress; A and B control the steady creep rate; considering the promoting effect of pre-deformation on the steady creep rate and balancing the monotonous enhancement of mathematical description for pre-deformation in Eq. (3), the impact factor of pre-deformation is described in Eq. (2). In addition, n_0 and n_1 show different effects of pre-deformation on different creep stages. Therefore, a unified creep constitutive model which can reflect the effects of aging system, stress levels and different pre-deformations has been established.

4.2 Determination of model constants for Al−Li−S4 alloy

It is difficult to well fit creep curves because of too many material constants required to calculate in the constitutive model. In order to acquire accurate constants, an intelligence algorithm, i.e., particle swarm optimization (PSO), is employed. The material constants are calculated and listed in Table 2. Figure 8 shows the comparison between calculated and experimental data. It can be seen from Fig. 8 that the modified constitutive model has a good ability to describe the primary and secondary creep stages of Al−Li−S4 alloy, and can well reflect the creep behaviors under different conditions.

Table 2 Creep-constitutive parameters for Al−Li−S4 alloy

A	B	σ_0/MPa	h	H^*	m_0
2.4967	0.0834	10.0830	228.2096	0.1413	3.0343
m_1	Q/(kJ·mol^{-1})	Y^*	n_0	n_1	
0.5674	57.6549	0.1328	2.7831	1.3333	

5 Conclusions

1) Comparing the creep results between samples with or without pre-deformation, it is obvious that the creep in the first stage is usually greater, and at 185 °C, 180 MPa and without pre-deformation the creep strain of the first stage even gets more than 70% of the total creep strain. Pre-deformation shortens the first creep stage obviously within the range of test parameters and decreases the total creep strain compared with samples without pre-deformation.

2) Compared with the creep results among samples with different pre-deformations, the first creep stage becomes shorter with the increase of pre-deformation

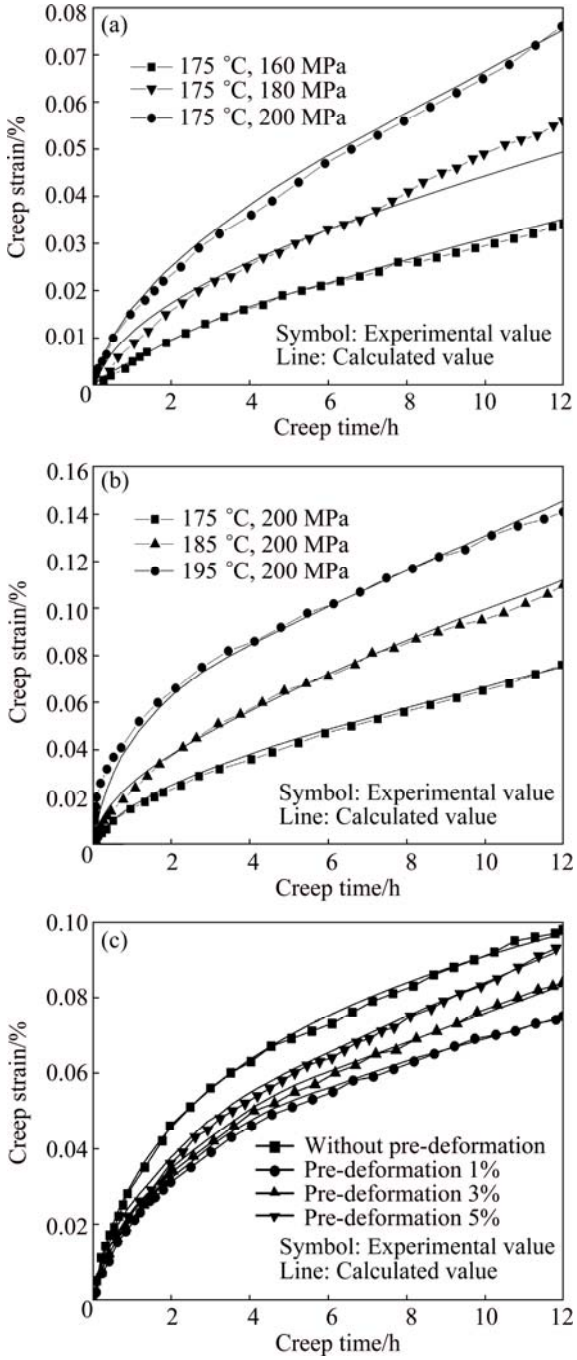

Fig. 8 Comparison between experimental and calculated creep strain values of Al−Li−S4 alloy under different conditions: (a) Under the same temperature, different stress levels and without pre-deformation; (b) Under the same stress, different temperatures and without pre-deformation; (c) Under 185 °C, 180 MPa and different pre-deformations

and the steady creep rate increases gradually. This effect raises the proportion of the second creep stage in the total process, and then the total creep strain rises. A large number of defects such as dislocations and vacancies produced by pre-deformation promote the second phase precipitating, which helps to hinder the dislocation motion. Meanwhile, pre-deformation brings about work-hardening which leads to the decrease of creep rate in the first stage. In the second creep stage as much more dislocations exist in the alloy, it is easy to generate dislocation slip and dislocation climb, thereby the steady creep rate rises.

3) Compared with the creep results, aging creep process has obvious strengthening effect on Al−Li−S4 alloy. The hardness and strength of the alloy go up gradually with the increase of pre-deformation, which is typical work-hardening phenomenon. On the other hand, more advantageous positions for the second-phase precipitating are provided by more dislocations and dislocation tangle, the volume fraction of precipitates in the alloy raises gradually, thus its conductivity rises.

4) θ' phase, $T1$ phase and δ' phase are observed in Al−Li−S4 alloy after aging creep. Pre-deformation significantly promotes finer $T1$ phase and θ' phase precipitating which distribute more dispersedly. The promotion for $T1$ phase is greater than that for θ' phase, and the larger the pre-deformation is, the higher the proportion of $T1$ phase in the alloy is. Even through the quantity and morphology of δ' phase cannot be influenced by pre-deformation, δ' phase dissolves because of the depletion of Li atoms by other phases. Besides, larger pre-deformation makes PFZ narrower and grain boundary chain-like precipitates distribute more and more continuously.

5) A unified creep constitutive model for Al−Li−S4 alloy which can reflect the effects of aging institution, stress levels and different pre-deformations has been established. The calculated results agree well with the experimental data.

References

[1] SALLAH M, PEDDIESON J, FOROUDASTAN S. A mathematical model of autoclave age forming [J]. Journal of Materials Processing Technology, 1991, 28(1−2): 211−219.

[2] LEQUEU P, LASSINCE P, WARNER T, RAYNARD G M. Engineering for the future: Weight saving and cost reduction initiative [J]. Aircraft Engineering and Aerospace Technology, 2001, 73(3): 147−159.

[3] ZHAN Li-hua, WANG Meng, HUANG Ming-hui Prediction model for aging stress-relaxation behavior based on creep equations [J]. Journal of Mechanical Engineering, 2013, 49(10): 70−76. (in Chinese)

[4] POLMEAR J I, PONS G, BARBAUX Y, OCTOR H, SANCHEZ C, MORTON J A, BORBIDGE E W, ROGERS S. After concorde: Evaluation of creep resistant Al−Cu−Mg−Ag alloys [J]. Materials Science and Technology, 1999, 15(8): 861−868.

[5] STARKE A E, STALEY T J. Application of modern aluminum alloys to aircraft [J]. Progress in Aerospace Sciences, 1996, 32(2−3): 131−172.

[6] ZENG Yuan-song, HUANG Xia. Forming technologies of large integral panel [J]. Acta Aeronautica et Astronautica Sinica, 2008, 29(3): 721−727. (in Chinese)

[7] LI Hui-zhong, ZHANG Xin-ming, CHEN Ming-an, ZHOU Zhuo-ping, GONG Min-ru. Effect of pre-deformation on microstructures and mechanical properties of 2519 aluminum alloy [J]. The Chinese Journal of Nonferrous Metals, 2004, 14(12): 1990−1994. (in Chinese)
[8] QUAN L W, ZHAO G, GAO S, MUDDLE C B. Effect of pre-stretching on microstructure of aged 2524 aluminium alloy [J]. Transactions of Nonferrous Metals Society of China, 2011, 21(9): 1957−1962.
[9] DECREUS B, DESCHAMPS A, DONNADIEU P, EEHRSTROM C J. On the role of microstructure in governing fracture behavior of an aluminum–copper–lithium alloy [J]. Materials Science and Engineering A, 2013, 586: 418−427.
[10] EMAMY M, RAZAHIAN A, KARSHENAS M. The effect of strain-induced melt activation process on the microstructure and mechanical properties of Ti-refined A6070 Al alloy [J]. Materials & Design, 2013, 46: 824−831.
[11] LI Hong-ying, SU Xiong-jie, LIN Hao, HUANG De-sheng. Microstructural evolution during homogenization of Al−Cu−Li−Mn−Zr−Ti alloy [J]. Transactions of Nonferrous Metals Society of China, 2013, 23(9): 2543−2550.
[12] LIN Yi, ZHANG Zi-qiao, ZHANG Hai-feng, HAN Ye. Effect of heat treatment process on tensile properties of 2A97 Al−Li alloy: Experiment and BP neural network simulation [J]. Transactions of Nonferrous Metals Society of China, 2013, 23(6): 1728−1736.
[13] FAN Mei-qiang, SUN Li-xian, XU Fen, MEI De-sheng, CHEN Da, CHAI Wen-xiang, HUANG Fen-lei, ZHANG Qing-ming. Microstructure of Al−Li alloy and its hydrolysis as portable hydrogen source for proton-exchange membrane fuel cells [J]. International Journal of Hydrogen Energy, 2011, 36(16): 9791−9798.
[14] GUPTA K R, NAYAN N, NAGASIREESHA G, SHARMA C S. Development and characterization of Al−Li alloys [J]. Materials Science and Engineering A, 2006, 420(1−2): 228−234.
[15] SUN Zhen-qi, HUANG Ming-hui. Effect of bonding on texture of Al−Li−S4 aluminum alloy [J]. Materials Science and Engineering of Powder Metallurgy, 2012, 17(4): 482−487. (in Chinese)
[16] RIOJA J R, LIU J. The evolution of Al−Li base products for aerospace and space applications [J]. Metallurgical and Materials Transactions A, 2012, 43(9): 3325−3337.
[17] LI Hua-guan, TAO Jie, SUN Zhong-gang, LIU Hong-bing, WANG Wen-tao, LUO Xin-yi. Effects of solution treatment on microstructure and properties of an aluminum−lithium alloy [J]. Heat Treatment of Metal, 2013, 38(3): 74−76. (in Chinese)
[18] WU Yao, XU Xiao-jing, ZHANG Zhen-qiang, SONG Tao, ZHANG Yun-kang, LUO Yong, DENG Ping-an. Solution treatment of 2099 Al−Li alloy with Sr and Sc additives [J]. Heat Treatment of Metal, 2013, 38(4): 40−44. (in Chinese)
[19] ZHAN Li-hua, LIN Jian-guo, DEAN A T, HUANG Ming-hui. Experimental studies and constitutive modeling of the hardening of aluminium alloy 7055 under creep age forming conditions [J]. International Journal of Mechanical Sciences, 2011, 53(8): 595−605.
[20] PAVLINA J E, van TYNE J C. Correlation of yield strength and tensile strength with hardness for steels [J]. Journal of Materials Engineering and Performance, 2008, 17(6): 888−893.
[21] DUMONT D, DESCHAMPS A, BRECHET Y. On the relationship between microstructure, strength and toughness in AA7050 aluminum alloy [J]. Materials Science and Engineering A, 2003, 356(1−2): 326−336.
[22] CAHOON R J, BROUGHTON H W, KUTZAK R A. The determination of yield strength from hardness measurements [J]. Metallurgical Transactions, 1971, 2(7): 1979−1983.
[23] CAI B, ADAMS L B, NELSON W T. Relation between precipitate-free zone width and grain boundary type in 7075-T7 Al alloy [J]. Acta Materialia, 2007, 55(5): 1543−1553.
[24] YOSHIMURA R, KONNOA J T, ABE E, HIRAGA K. Transmission electron microscopy study of the early stage of precipitates in aged Al−Li−Cu alloys [J]. Acta Materialia, 2003, 51(10): 2891−2903.
[25] GLADMAN T. Precipitation hardening in metals [J]. Materials Science and Technology, 1999, 15(1): 30−36.
[26] KOWALEWSKI L Z, HAYHURST R D, DYSON F B. Mechanisms-based creep constitutive equations for an aluminium alloy [J]. Journal of Strain Analysis for Engineering Design, 1994, 29(4): 309−316.
[27] LI Chao, WAN Min, WU Xiang-dong, HUANG Lin. Constitutive equations in creep of 7B04 aluminum alloys [J]. Materials Science and Engineering A, 2010, 527(16−17): 3623−3629.
[28] LIN J, HO C K, DEAN A T. An integrated process for modelling of precipitation hardening and springback in creep age-forming [J]. International Journal of Machine Tools and Manufacture, 2006, 46(11): 1266−1270.
[29] KOLAR M, PEDERSEN O K, GULBRANSEN-DAHL S, TEICHMANN K, MARTHINSEN K. Effect of pre-deformation on mechanical response of an artificially aged Al−Mg−Si alloy [J]. Materials Transactions, 2011, 52: 1356−1362.

预变形对 Al−Li−S4 合金时效蠕变的影响规律及其本构建模

王 萌[1,2]，湛利华[1,2]，杨有良[1,2]，阳 凌[1,2]，黄明辉[1,2]

1. 中南大学 机电工程学院，长沙 410083；2. 中南大学 高性能复杂制造国家重点实验室，长沙 410083

摘 要：以 Al−Li−S4 合金为研究对象，开展其在不同预变形量、不同时效温度和试验应力下的单向拉伸蠕变试验，获得 Al−Li−S4 合金在时效成形基本热力条件下的时效蠕变行为和预变形对其形变、力学性能和显微组织的影响规律。结果表明：试样预变形量越大，蠕变第一阶段持续时间越短，蠕变第二阶段的稳态蠕变速率越大，最终的蠕变应变量越大，但在试验参数范围内仍小于未经预变形处理试样的蠕变应变量；TEM 结果显示，引入预变形对 T_1 相和 θ'相析出有一定的促进作用并能显著促进析出相的细小弥散分布，同时抑制 δ'相的析出，从而改善合金的力学性能。建立了能够反映时效机制、应力和预变形影响的蠕变时效统一本构模型，该模型的拟合结果对实验数据有较好的回归效果。

关键词：Al−Li−S4 合金；时效蠕变；预变形；力学性能；显微组织；本构模型

(Edited by Wei-ping CHEN)